European Heart Journal (2017) **38**, 400–412
doi:10.1093/eurheartj/ehw097

REVIEW

Imaging

Hybrid intravascular imaging: recent advances, technical considerations, and current applications in the study of plaque pathophysiology

Christos V. Bourantas[1], Farouc A. Jaffer[2], Frank J. Gijsen[3], Gijs van Soest[3], Sean P. Madden[4], Brian K. Courtney[5], Ali M. Fard[6], Erhan Tenekecioglu[3], Yaping Zeng[3], Antonius F.W. van der Steen[3], Stanislav Emelianov[7], James Muller[4], Peter H. Stone[8], Laura Marcu[9], Guillermo J. Tearney[6], and Patrick W. Serruys[3,10]*

[1]Department of Cardiovascular Sciences, University College London, London, UK; [2]Cardiovascular Research Center and Cardiology Division, Harvard Medical School and Massachusetts General Hospital, Boston, MA, USA; [3]Thorax Center, Erasmus MC, 's-Gravendijkwal 230, 3015 CE Rotterdam, The Netherlands; [4]InfraReDx, Inc., Burlington, MA, USA; [5]Sunnybrook Health Sciences Centre, University of Toronto, Toronto, Canada; [6]Wellman Center for Photomedicine, Harvard Medical School and Massachusetts General Hospital, Boston, MA, USA; [7]Department of Biomedical Engineering, University of Texas at Austin, Austin, TX, USA; [8]Cardiovascular Division, Brigham & Women's Hospital, Harvard Medical School, Boston, MA, USA; [9]Department of Biomedical Engineering, University of California, CA, USA; and [10]International Centre for Cardiovascular Health, NHLI, Imperial College London, London, UK

Received 13 September 2015; revised 31 January 2016; accepted 22 February 2016; online publish-ahead-of-print 26 April 2016

Cumulative evidence from histology-based studies demonstrate that the currently available intravascular imaging techniques have fundamental limitations that do not allow complete and detailed evaluation of plaque morphology and pathobiology, limiting the ability to accurately identify high-risk plaques. To overcome these drawbacks, new efforts are developing for data fusion methodologies and the design of hybrid, dual-probe catheters to enable accurate assessment of plaque characteristics, and reliable identification of high-risk lesions. Today several dual-probe catheters have been introduced including combined near infrared spectroscopy-intravascular ultrasound (NIRS-IVUS), that is already commercially available, IVUS-optical coherence tomography (OCT), the OCT-NIRS, the OCT-near infrared fluorescence (NIRF) molecular imaging, IVUS-NIRF, IVUS intravascular photoacoustic imaging and combined fluorescence lifetime-IVUS imaging. These multimodal approaches appear able to overcome limitations of standalone imaging and provide comprehensive visualization of plaque composition and plaque biology. The aim of this review article is to summarize the advances in hybrid intravascular imaging, discuss the technical challenges that should be addressed in order to have a use in the clinical arena, and present the evidence from their first applications aiming to highlight their potential value in the study of atherosclerosis.

Keywords Intravascular imaging • Coronary atherosclerosis • Hybrid imaging

Introduction

Intravascular imaging was introduced in the clinical setting in the beginning of 1990s and enabled for the first time *in vivo* evaluation of the atheroma burden and detection of plaque characteristics associated with increased vulnerability.[1] The first clinical applications of intravascular imaging techniques [i.e. intravascular ultrasound (IVUS) and optical coherence tomography (OCT)] demonstrated their potential value in assessing plaque morphology and pathophysiology and generated optimism that intravascular imaging would enable accurate detection of high-risk plaques likely to cause clinical events.[2,3] However, recent histology-based studies and large-scale studies of coronary atherosclerosis revealed significant limitations of existing imaging modalities in detecting vulnerable plaque characteristics and high-risk lesions (i.e. in the PROSPECT study the positive predictive value of IVUS-derived variables in detecting lesions that caused events was 18.2% while in the PREDICTION the positive predictive value of IVUS-derived variables and of the local haemodynamic forces in detecting lesions that progressed and required revascularization was 41%) and

* Corresponding author. Tel: +31 10463 5260, Fax: +31 10436 9154, Email: patrick.w.j.c.serruys@gmail.com

highlighted the need to design alternative invasive imaging techniques that would allow complete and accurate evaluation of plaque morphology and pathobiology.[4–7]

The miniaturization of medical devices and advances in image and signal processing permitted the development of novel modalities [e.g. near infrared spectroscopy (NIRS), intravascular photoacoustic (IVPA) imaging, near infrared fluorescence (NIRF) molecular imaging, and time-resolved fluorescence spectroscopy (TRFS), or fluorescence lifetime imaging (FLIm)] that appear able to address certain limitations of either IVUS or OCT and provide additional information about plaque morphology and pathobiology. Nevertheless, no single existing technique enables a complete assessment of the plaque (Supplementary material online, file). To address this challenge, hybrid imaging has been suggested. Hybrid intravascular imaging can be obtained either through the development of methodologies that allow reliable offline co-registration of data acquired by different modalities with complementary strengths, or through the design of dual-probe catheters that enable simultaneous assessment of plaque morphology by two different imaging techniques.[8] Over the recent years, significant advances have occurred in this field and accumulating evidence indicates the potential value of hybrid imaging in research. The aim of this article is to present the latest developments in hybrid intravascular imaging, describe the technical challenges and limitations of the available data fusion methodologies and dual-probe catheters, summarize the evidence from their first applications, and discuss their future role in the study of coronary atherosclerosis (*Table 1*).

Recent advances in hybrid intravascular imaging modalities

Fusion of intravascular and X-ray imaging data

The first methodologies developed to reconstruct the three-dimensional (3D) coronary artery anatomy from IVUS and X-ray angiographic data required prospective image acquisition and the implementation of tedious protocols (i.e. the use of calibration objects, and simultaneous imaging of the IVUS catheter and the luminal silhouette) that restricted considerably their applications in research.[9–11] These limitations were overcome by a recently introduced approach that has the ability to retrospectively reconstruct the coronary anatomy from routine coronary angiography and IVUS,[12]and it has already been used to study the effect of the local haemodynamic forces on plaque growth (*Figure 1*).[13]

Numerous *in vivo* studies have shown that low and oscillating endothelial shear stress (ESS) determine plaque evolution and vulnerable plaque formation while the PREDICTION study, the largest study of its kind, demonstrated that low ESS is an independent predictor of future revascularizations.[7,14,15] In addition, IVUS-based modelling has been used to examine the implications of the ESS on neointimal proliferation, while a recent IVUS-virtual histology (VH)-based study has shown that ESS affects also neointima composition.[13,16] Nevertheless IVUS-based modelling cannot provide detailed reconstruction of the lumen surface in stented/scaffolded segments and in ruptured plaques as IVUS imaging has limited resolution which does not permit detailed visualization of the luminal surface and of the struts.

These limitations have been recently addressed by OCT-based modelling. Three methodologies are today available for the reconstruction of the coronary anatomy from X-ray and OCT data (*Figure 1*).[17–19] Applications of these techniques have shown that the high resolution of OCT enables more detailed reconstruction of luminal morphology and of the protruded struts in scaffolded segments, reliable evaluation of the flow disturbances and recirculation zones (Supplementary material online, *Figure S5*), and assessment of the association between neointimal proliferation and ESS.[20] OCT-based modelling has also been used to evaluate the association between ESS and plaque micro-features that cannot be visualized by IVUS such as macrophages, micro-calcifications, and neo-vessels.[21] In a small-scale study that included 21 patients admitted with an acute coronary syndrome, low ESS was associated with an increased incidence of OCT-derived thin-cap fibroatheromas (TCFA), spotty calcifications, macrophage accumulation and thinner fibrous caps over necrotic cores, while another report has shown that high ESS was seen more often at the rupture site and was associated with an increased lipid component, and thinner fibrous caps.[22] These findings support hypotheses and previous experimental studies which advocate that low ESS promotes vulnerable plaque formation and destabilization, while high ESS likely contributes to the specific location of frank plaque rupture.[23,24]

Fusion of intravascular imaging and computed tomographic coronary angiography

The first method to fuse non-invasive, computed tomography coronary angiography (CTCA) with IVUS data was introduced by van der Giessen *et al.*[25] The proposed approach is similar to methodologies proposed to fuse X-ray and intravascular imaging and combines 3D centreline data from CTCA and anatomical landmarks seen on both IVUS and CTCA to identify the position and orientation of IVUS images onto the extracted centreline. IVUS-CTCA-derived models appear an attractive alternative for ESS computation, especially since it is easier to study coronary artery bifurcations.[26] Combined CTCA and IVUS imaging demonstrated that plaques in coronary bifurcations are exposed to increased ESS even from the early stages of plaque development, and that high ESS associate with the location of plaque rupture.[27] In a small CTCA-IVUS study, low ESS was associated with thicker plaques, containing predominantly IVUS-derived fibrofatty tissue.[28] Recently, fusion of CTCA and IVUS was used to simulate a stent deployment procedure.[29] Both the lumen and the vessel wall of a coronary bifurcation were reconstructed, and numerical procedures were applied to model stent deployment. This feasibility study demonstrated the potential of *in silico* methodologies to plan and optimize stenting in complex procedures.

An identical methodology can be applied to fuse OCT and CTCA data. Recently, Karanasos *et al.* fused CTCA and IVUS, and CTCA and OCT data to investigate the relationship between ESS and fibrous cap thickness in segments implanted with bioresorbable scaffolds.[30] They demonstrated that high ESS, 2 years post-implantation,

Table 1 Advantages and limitations of the existing invasive imaging modalities and the available hybrid imaging techniques

Imaging modalities	Features associated with increased plaque vulnerability							Fast analysis	Current status
	Lumen dimensions	Plaque burden and positive remodelling	Lipid component	Cap thickness	Neo-angiogenesis	Inflammation	ESS assessment		
IVUS + X-ray	+++	+++	+	+	−	−	+++	−	Extensive applications in the study of the role of ESS in atherosclerotic evolution
OCT + X-ray	+++	+	++	+++	++	+	+++	−	Extensive applications in the study of the role of ESS in atherosclerotic evolution
IVUS + CTCA	+++	+++	+	+	−	−	+++	−	Implemented to evaluate the efficacy of CTCA in assessing plaque morphology
OCT + CTCA	+++	+	++	+++	++	+	+++	−	Limited applications in the study of the association between plaque characteristics and the local haemodynamic forces
NIRS-IVUS	+++	+++	+++	++	−	−	−	++	Commercially available
IVUS-OCT	+++	+++	++	+++	++	+	−	+	*In vivo* validation
OCT-NIRF	+++	+	++	+++	++	+++	−	NK	First in man studies
IVUS-NIRF	+++	+++	+	+	−	+++	−	NK	Under development
OCT-NIRS	+++	+	+++	+++	++	+	−	NK	*Ex vivo* validation
IVUS-IVPA	+++	+++	++	+	+	++	−	NK	*Ex vivo* validation
IVUS-FLIm	+++	+++	++	+++	−	++	−	NK	*In vivo* validation

(+++) indicates excellent performance of the modality; (++) moderate performance of the modality; (+) poor performance of the modality; (−) the modality is unable to provide this information; (NK) not known.
EES, endothelial shear stress; IVUS, intravascular ultrasound; RF-IVUS, radiofrequency analysis of the IVUS backscattered signal; OCT, optical coherence tomography; NIRS, near infrared spectroscopy; CTCA, computed tomographic coronary angiography; NIRF, near infrared fluorescence imaging; IVPA, intravascular photoacoustic imaging; FLIm, fluorescence life time imaging.

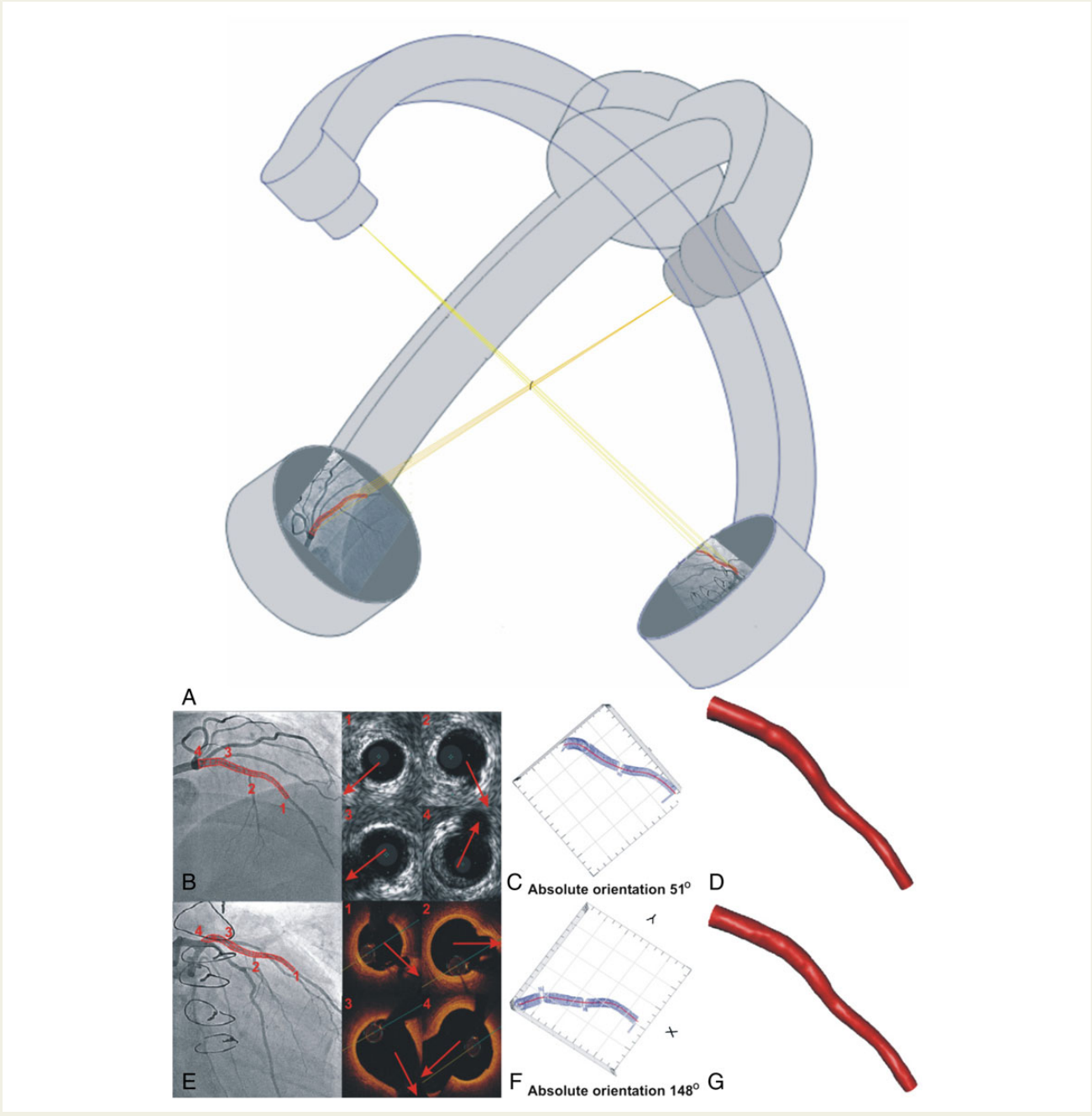

Figure 1 Centreline methodology proposed to reconstruct coronary anatomy from X-ray and intravascular imaging data acquired during a conventional cardiac catheterization. The luminal centreline is detected in two angiographic projections and then it is extruded perpendicularly to its plane forming two surfaces (*A*). The intersection of the two surfaces is a 3D curve that corresponds to the backbone of the vessel. The side branches are identified in the intravascular ultrasound or the optical coherence tomography images and vectors are drawn to mark their direction (Panels 1, 2, 3, 4). These vectors and the luminal borders detected in the remaining frames are placed perpendicularly onto the extracted luminal centreline and their relative axial twist is estimated using the sequential triangulation algorithm. The first intravascular ultrasound or optical coherence tomography frame is rotated around the luminal centreline, the reconstructed lumen is projected onto the angiographic images and the direction of the vectors indicating the side branches in intravascular images are compared with the origin of the corresponding branches in X-ray projections (*B* and *E*). The rotation angle of the first frame at which the best matching is achieved corresponds to the correct absolute orientation of the first frame (*C*–*F*). The final intravascular ultrasound - and optical coherence tomography-based models are shown in panels (*D*–*G*). The data for the design of this figure were kindly provided by Jang.

Table 2 Technical characteristics of the combined intravascular imaging catheters

Imaging modality	Probe size	Probe arrangement	Probe characteristics[a]	Image depth	Image axial resolution	Frame rate	Technical limitations restricting clinical applications	Histological evidence
NIRS-IVUS	3.2 Fr	IVUS transducer and NIRS optics at 180° apart	NIRS: 800–2500 nm IVUS: 50 MHz	NIRS: <3 mm IVUS: 16 mm	IVUS: 20 μm	NIRS: 150 spectra/s IVUS: 16/s	None	The NIRS ability to detect lipid core was 86% in the only prospective validation study of its kind[31]
IVUS-OCT	7.2 Fr[37]	Side by side	IVUS: 40 MHz OCT: 1310 nm	NA	IVUS: 38 μm OCT: 8 μm	1/s	Large catheter size Poor image quality Low image acquisition rate	*In vitro* feasibility study in a rabbit aorta
	4 Fr[38]	Side by side 90° apart	IVUS: 42.5 MHz OCT: 1325 nm	OCT: 1 mm within tissue	NA	5/s	Increased artefacts/ moderate image quality Low frame rate Poor co-registration in case of NURD	Qualitative validation in human cadavers
	3.6 Fr[39]	Sequential arrangement –2 mm apart	IVUS: 35 MHz OCT: NA	IVUS: 4.5 mm OCT: NA	IVUS: 60 μm OCT: 8 μm	20/s	Large catheter size Inaccurate co-registration of IVUS and OCT	Feasibility study in human cadaver and *in vivo* in the aorta of a rabbit
	2.7 Fr[40,*]	Back to back	IVUS: 45 MHz OCT: NA	NA	NA	10/s	Low image acquisition rate	Feasibility study in human and swine cadavers
	3 Fr	Co-linear ultrasound and optical beams	IVUS: 40 MHz OCT: 1320 nm	NA	NA	100/s	None	Feasibility in pre-clinical *in vivo* models
OCT-NIRF	2.4 Fr[44]	Dual clad fibre with a single-mode OCT core and an inner NIRF cladding	OCT: 1320 nm NIRF: 750 nm	NIRF: 3 mm	OCT: 7 μm	25.4/s	Low image acquisition rate	Feasibility study in cadaveric human coronary artery and *in vivo* in rabbits
	2.6 Fr[45]	Dual clad fibre with a single mode OCT core and an inner NIRF cladding	OCT: 1290 nm NIRF: 749–790 nm	OCT: 1–2 mm	OCT: 7 μm	100/s	None	Feasibility study *in vivo* in rabbit models
IVUS-NIRF	4.2 Fr[52]	Side by side	IVUS: 45 MHz NIRF: 750 nm	IVUS: 4 mm NIRF: 2 mm	IVUS: NA	30/s	Large size catheter	*In vitro* validation in phantoms and feasibility study *ex vivo* in porcine carotids
OCT-NIRS	2.4 Fr[53]	Side by side	OCT: 1282 nm NIRS: 1230–1330 μm	OCT: 1.5 mm	OCT: 10 μm	24/s	None	Feasibility study in a cadaveric human coronary artery
IVUS-IVPA	3.6 Fr[56]	Parallel alignment	IVUS: 35 MHz IVPA: 532 μm	IVUS: 5 mm	IVUS: 59 μm	NA	The need for blood removal for IVPA imaging	*In vitro* validation in a wire phantom model and a feasibility study in a rabbit aorta
	3.6 Fr[56]	Parallel alignment	IVUS: 80 MHz IVPA: 532 μm	IVUS: 4 mm	IVUS: 35 μm	NA	The need for blood removal for IVPA imaging	*In vitro* validation in a wire phantom model and a feasibility study in a rabbit aorta
	8.7 Fr[58]	IVPA probe within the IVUS probe	IVUS: 35 MHz IVPA: 1197 μm	NA	NA	1/s	Large catheter size The increased time needed for IVPA imaging	*In vitro* validation in phantom models and a feasibility study in a pig iliac artery

Continued

Table 2 *Continued*

Imaging modality	Probe size	Probe arrangement	Probe characteristics[a]	Image depth	Image axial resolution	Frame rate	Technical limitations restricting clinical applications	Histological evidence
	2.7 Fr[57]	Sequential arrangement	IVUS: 40 MHz IVPA: 1210 μm	IVUS: 4.5 mm IVPA: 4.5 mm	IVUS: 100 μm IVPA: 100 μm	5/s	The increased time required for IVPA imaging	*In vitro* validation in phantom models and a feasibility study in a stented rabbit iliac artery
IVUS-FLIm	7 Fr[66]	Side by side	IVUS: 40 MHz FLIm: 300 μm	NA	NA	FLIm: 6.7/s IVUS: 30/s	Large catheter size The need for balloon inflation to obstruct flow	Feasibility study *in vivo* in the femoral artery of a pig model
	5 Fr[67]	Side by side	IVUS: 40 MHz FLIM: 390–629 μm	NA	FLIm: 160 μm	IVUS: 30/s FLIm: 40/s	The need for blood flow obstruction Inaccurate co-registration of FLIm and IVUS data The offline analysis of the FLIm data	*Ex vivo* validation in cadaveric coronary arteries (sensitivity and specificity range: 84–100% for all plaque types) and in a swine coronary arteries[68]

NIRS, near infrared spectroscopy; IVUS, intravascular ultrasound; OCT, optical coherence tomography; NA, not available; NURD, non-uniform rotational distortion; NIRS, near infrared spectroscopy; NIRF, near infrared fluorescence imaging; IVPA, intravascular photoacoustic imaging; FLIm, fluorescence life time imaging.
[a]All the multimodality imaging probes incorporated a rotational IVUS transducer.
* The diameter of this prototype does not include the sheath that would protect the the rotating housing from the artery.

was correlated to thicker fibrous caps at 5 years, indicating that ESS modulates the long-term vascular healing response of the vessels treated with these devices.

Combined near infrared spectroscopy-intravascular ultrasound imaging

Combined NIRS-IVUS imaging is the only hybrid intravascular imaging technology currently approved for clinical use in the USA and other countries and was introduced in order to provide more reliable assessment of plaque morphology and composition. The combination of NIRS and IVUS in a simultaneously acquired and co-registered manner is particularly advantageous, since IVUS can measure plaque structure, while NIRS accurately and reproducibly can determine the presence of lipid-rich plaques.[31] Currently, commercially available NIRS-IVUS combines extended bandwidth 50 MHz rotational IVUS with NIRS on a single 3.2 Fr monorail catheter (*Table 2*).

Near infrared spectroscopy-intravascular ultrasound has been used in a number of trials to assess the effect of statins on plaque burden and composition.[32,33] Near infrared spectroscopy-intravascular ultrasound studies have also shown that the culprit lesions in patients with non-ST or ST elevation myocardial infarction have specific morphological characteristics (i.e. an increased lipid component and plaque burden), suggesting that a high-risk lipid plaque signature is associated with acute cardiac events (*Figure 2*).[34,35] Some early results suggest the ability of NIRS-IVUS to identify plaque characteristics associated with future events,[36] and two major trials are underway (Prospect II, NCT02171065; and the Lipid Rich Plaque Study, NCT02033694) to more comprehensively and rigorously prove this hypothesis.

Limitations of NIRS-IVUS include the inadequate resolution of IVUS for finer measurements such as the neointimal coverage of stent struts or the cap thickness, the loss of the IVUS imaging signal behind calcific tissue or stent struts, occasional lumen border definition issues in the presence of thrombus or high blood speckle, and the requirement to prime and sometimes flush the imaging catheters. Near infrared spectroscopy is limited by not giving explicit depth information of the lipid core plaque, and thus superficial lipid cannot be distinguished from deep lipid in the same arc using the NIRS information alone.

Combined intravascular ultrasound-optical coherence tomography imaging

Of the existing intravascular imaging modalities developed thus far, the two technologies with the largest collections of published literature and clinical experience are IVUS and OCT. Intravascular ultrasound has the advantages of a large field of view, deeper imaging depth and the ability to see through blood, while OCT has better contrast than IVUS between soft plaque components, such as lipid-rich regions, fibrous tissue, and thrombus. Optical coherence tomography has also better resolution at the expense of poorer imaging depth that often precludes assessment of the atheroma burden and remodelling pattern.

In light of the complementary nature of IVUS and OCT, several probes combining the two modalities have been developed and tested in *ex vivo* and pre-clinical *in vivo* settings (*Table 2*). The first such published report in 2010 was done on a bench-top setting

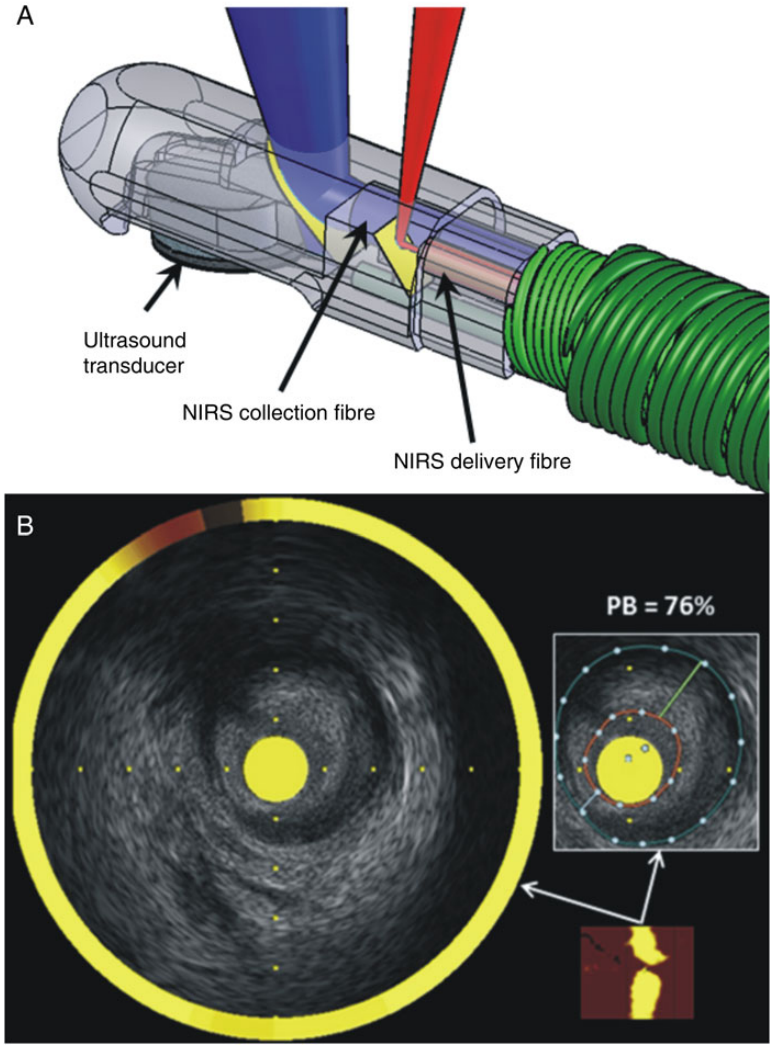

Figure 2 Combined near infrared spectroscopy—intravascular ultrasound catheter. (*A*) The tip of the catheter incorporates a rotating intravascular ultrasound transducer operating at 50 MHz with extended bandwidth, and two near infrared spectroscopy fibres that transmit and collect the near infrared light. (*B*) The chemogram is the output of the near infrared spectroscopy catheter (bottom right), is co-registered with the intravascular ultrasound data creating hybrid images that allow assessment of lumen, outer vessel wall, and plaque dimensions including plaque burden and simultaneous evaluation of the longitudinal and circumferential distribution of the lipid component. Panel B was reprinted with permission from Madder *et al.*[35]

with a rigid 7.2 Fr probe that could rotate at 1 rotation per second.[37] Subsequently, the feasibility of a hybrid IVUS-OCT imaging assembly was implemented in a 4 Fr flexible catheter and tested on human cadaver specimens.[38] The OCT and IVUS beams in this implementation scanned the same cross-section of tissue, but they were fixed at 90° apart from each other, thus potentially subjecting the co-registration of the two images to inaccuracy in the event of non-uniform rotational distortion. The first reported *in vivo* pre-clinical IVUS-OCT imaging was acquired using a 3.6 Fr catheter in a rabbit aorta where the IVUS and OCT beams were separated from each other by 2 mm along the length of the catheter.[39] In order to minimize loss of co-registration caused by cardiac motion during pull-back, a new 'back-to-back' design was built wherein the IVUS and OCT beams were 180° apart from each other, but without any longitudinal offset.[40] More recently, a 3 Fr hybrid IVUS-OCT catheter with a guidewire tip was built wherein the optics reside within the ultrasound transducer to facilitate miniaturization, while the IVUS and OCT beams travel in the same direction (*Figure 3*). This design eliminates any rotational or longitudinal offset between the two modalities that may occur, thus eliminating co-registration artefacts due to cardiac motion or variations in the rotational motion of the imaging assembly. Finally, a probe that combines the imaging depth of IVUS, the resolution of OCT, and fluorescence imaging for plaque characterization has been tested *ex vivo*.[41] This latter tri-modality probe was implemented with a 3.6 Fr diameter imaging assembly in the absence of a catheter sheath.

While progress continues on the miniaturization, co-registration and imaging performance of hybrid IVUS-OCT probes, demonstration

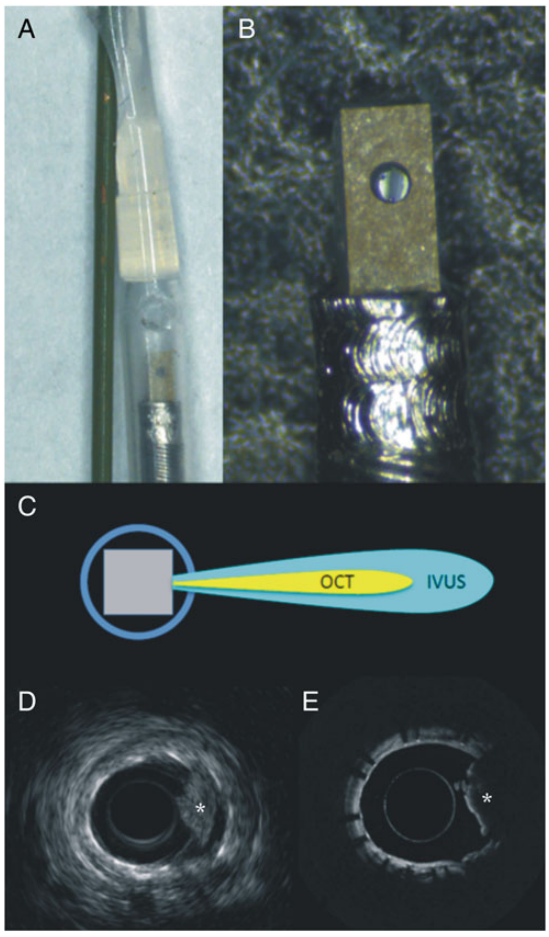

Figure 3 Dual mode intravascular ultrasound—optical coherence tomography catheter. The prototype has a diameter of 3 Fr with the optical coherence tomography component being integrated to the intravascular ultrasound probe (*A* and *B*). This design allows a collinear alignment of the two transducers (*C*), and thus accurate co-registration of the intravascular ultrasound (*D*) and optical coherence tomography (*E*) images (the asterisk indicates the presence of red thrombus).

of the use of such a technology in human patients has not yet occurred, but is anticipated with a real-time image acquisition and display system in the near future (2016). Data continue to emerge with respect to the hypothetical benefits of such a combination in characterizing the composition of the plaque[42] creating promise that combined IVUS-OCT imaging will provide more accurate assessment of plaque evolution, and quantification of the effect of new treatments on plaque progression.

Combined near infrared fluorescence molecular imaging

Optical coherence tomography-near infrared fluorescence imaging

Atherosclerosis and stent complications are driven by their underlying pro-inflammatory and pro-thrombotic biological milieu. Molecular, or biological imaging is a relatively new field that aims to image molecular and cellular details in living subjects through injectable, specialized imaging agents followed by matched imaging systems. Near infrared fluorescence molecular imaging is a clinically translatable approach that allows intravascular imaging of biological detail in coronary arteries.[43]

Recognizing the need to co-register structural arterial information and NIRF information, a hybrid-dual modal OCT-NIRF system was constructed and validated *in vivo*.[44] This system employs a 2.4 Fr imaging device based on a clinical standalone OCT platform, and in addition to enabling exact co-registration of the 750 nm NIRF and 1320 nm OCT signals, it enables distance-corrected NIRF signal quantification exactly co-registered with OCT-depicted anatomy (*Table 2*). The NIRF signal is not axially resolved, as fluorescence is an incoherent phenomenon, and thus the NIRF signal is typically displayed on the luminal surface of the vessel wall. The OCT-NIRF system has recently demonstrated the ability to image and quantify plaque inflammation (augmented NIRF cysteine protease activity) *in vivo* in rabbit models with simultaneous mapping of plaque structure by OCT (*Figure 4*).

A similar dual-probe OCT-NIRF catheter has been designed by Lee *et al.*[45] The prototype has diameter of 2.6 Fr and can acquire images at a rate of 100 frames/s via automated pull-back up to a maximum speed of 40 mm/s. *In vivo* validation demonstrated the efficacy of the catheter to detect indocyanine green deposition in macrophage-rich rabbit atheroma, confirming the findings of Vinegoni *et al.*[46] Indocyanine green, a clinically approved agent, has recently further been shown to target human carotid plaques, and should accelerate intracoronary NIRF molecular imaging trials.[47]

The ability of NIRF to image molecules associated with plaque inflammation could enhance the identification of plaques at risk for progression and complication, and synergize with structural imaging methods such as OCT. In addition, because NIRF systems can detect a diverse array of NIRF imaging agents, intravascular NIRF molecular imaging can report on plaque protease activity, plaque macrophages, abnormal endothelial permeability, and fibrin deposition on stents (Video).[48,49] Translationally, clinical intracoronary NIR fluorescence-OCT imaging has recently been demonstrated via detection of plaque 633 nm NIR autofluorescence (NIRAF) in human coronary arteries, as discussed in the next section.[50] This is important step towards enabling targeted NIRF molecular imaging in the 750–800 nm excitation range.

Optical coherence tomography-near infrared autofluorescence imaging

Autofluorescence patterns of atheroma may provide insights into plaque composition, as evidenced by extensive work in time-resolved fluorescence detection in the UV and visible light range. Recently, Wang *et al.* has demonstrated 633 nm-excited autofluorescence, detected in the NIR (700–900 nm).[51] This NIRAF signal was measured in human cadaver plaques and found to be highest in necrotic cores identified by histology. When combined with OCT, this device could improve our capability to reliably detect TCFA.

Intravascular ultrasound-near infrared fluorescence imaging

As NIR light can travel efficiently through blood, it is in fact possible to perform NIRF molecular imaging through blood in coronary

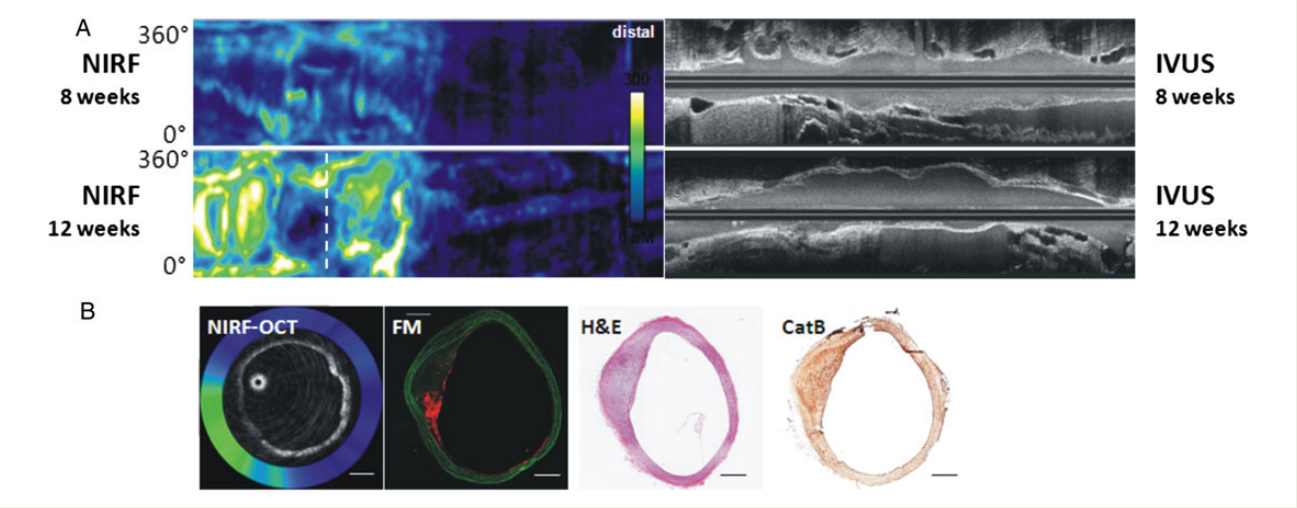

Figure 4 Serial optical coherence tomographic—near infrared fluoresence imaging of plaque inflammation with the ProSenseVM110, a molecular sensor for cathepsin protease activity. Atheroma was induced in the rabbit aorta by mechanical balloon injury and hypercholesterolaemic diet. Serial *in vivo* optical coherence tomographic—near infrared fluoresence and intravascular ultrasound imaging was performed at 8 and 12 weeks after injury, 24 h after intravenous injection of ProSenseVM110. (*A*) Longitudinal co-registered near infrared fluorescence and intravascular ultrasound imaging at 8 and 12 weeks. (*B*) Axial optical coherence tomographic—near infrared fluorescence fusion image (yellow/white = high near infrared fluorescence; blue/black = low near infrared fluorescence) at the location of the white dotted line in (*A*), second row (near infrared fluorescence, 12 weeks). Matched cross-sectional fluorescence microscopy (red = ProSense VM110; green = autofluorescence) and histopathology demonstrates increased ProSense VM110 NIRF signal within a moderate fibrofatty atheroma (H&E) associated with cathepsin B immunostain. Scale bars, 1 mm. Figure courtesy of Dr Eric Osborn and Dr Giovanni Ughi.

arteries.[43] Therefore, integrating NIRF with IVUS is attractive as IVUS is performed through blood, and IVUS remains the most widely utilized intravascular imaging approach currently. A 1.4 mm (4.2 Fr) IVUS-NIRF catheter has been described by Dixon and Hassock for *ex vivo* intravascular imaging (*Table 2*).[52] Newer solutions will attempt to miniaturize the device to <3 Fr diameter suitable for intracoronary use *in vivo*, and to better reconstruct fluorescence light attenuated by blood.

Combined optical coherence tomography-near infrared spectroscopy imaging

Even though microstructural imaging provides unique insights about plaque pathology, advancing understanding and improving diagnosis of high-risk lesions require knowledge of the artery's chemical and molecular composition. While some chemical data, such as the presence of lipid, may be inferred from OCT signal, this information is limited to the imaging depth of OCT, which may be superficial, especially in the presence of macrophages and lipid.

Recently, a dual-modality OCT-NIRS catheter was developed that integrates the two modalities using a two-fibre arrangement (*Table 2*).[53] The catheter illuminates the tissue through a single-mode fibre and collects the backscattered OCT light with the same fibre. A second collection fibre within the catheter enables a source-detector separation that allows chemical sensing to be performed deeper into the artery walls, as the detected signal travels over longer path lengths. The OCT-NIRS system utilizes a wavelength-swept light source for both OCT and NIRS modalities.

A schematic of the distal tip of the OCT-NIRS catheter is shown in *Figure 5A*, while *Figure 5B* and *C* illustrate the potential value of combined OCT-NIRS imaging in characterizing the composition of the plaque. Although OCT images appear similar, NIRS data (shown as normalized attenuation spectra in the ring around the OCT image) identified lipid only in the lesion in *Figure 5C* indicating the presence of a fibrocalcific plaque in *Figure 5B*. These results demonstrate that catheter-based OCT-NIRS imaging provides complementary structural and compositional data that may be used to enhance our capability for detecting fibroatheroma in humans.

Near infrared spectroscopy combined with OCT to probe spectral features of additional plaque molecules will therefore: (i) make it easier for non-expert OCT readers to delineate fibroatheromas, (ii) enable the correlation between lipid content and OCT microstructural features, and (iii) facilitate automated segmentation of lipid-containing lesions. Future directions include development of a broad bandwidth cholesterol to cholesterol esters ratio that is known to be associated with high-risk coronary lesions.

Combined intravascular ultrasound-intravascular photoacoustic imaging

Intravascular photoacoustic imaging is an analytical chemistry diagnostic technique which appears able to characterize the depth-resolved composition of atherosclerotic plaques, specifically lipids such as cholesterol esters. Intravascular photoacoustic images provide chemical information about plaque composition, can detect the stent struts, and are inherently collocated with tissue structure obtained by IVUS, as the same transducer can be used to perform a

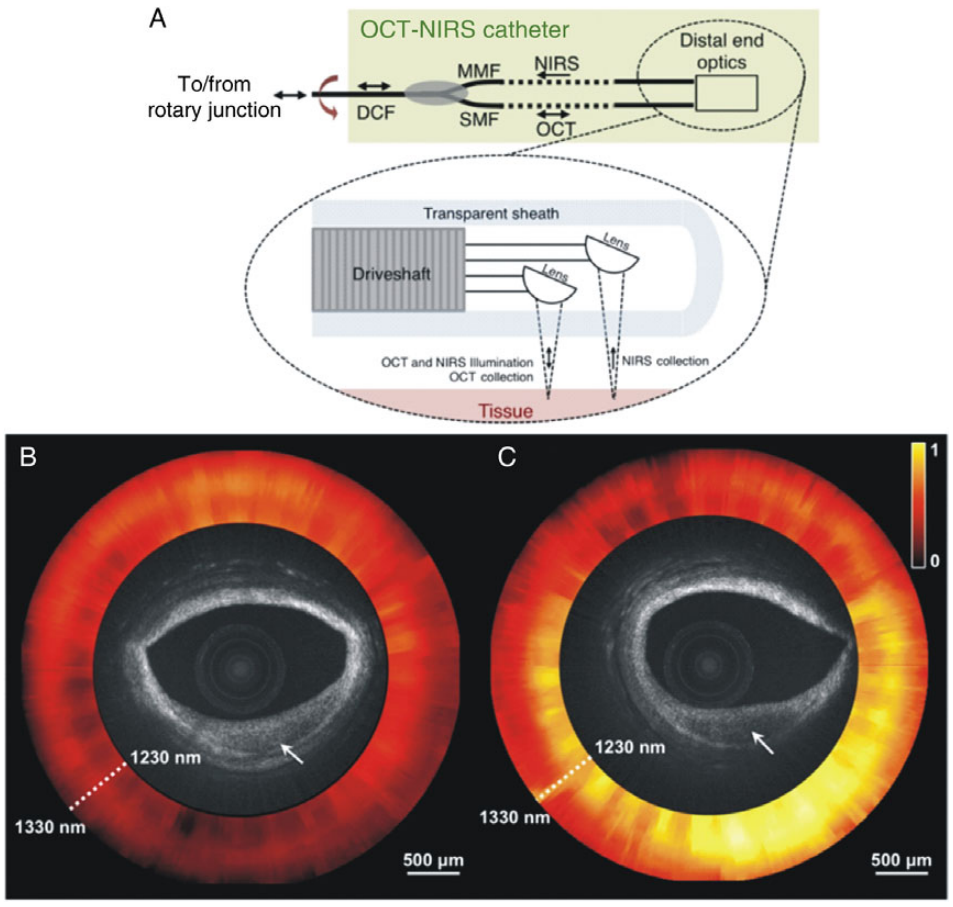

Figure 5 Schematic representation of the combined optical coherence tomography—near infrared spectroscopy catheter (*A*). Optical coherence tomography—near infrared spectroscopy images of human cadaver plaques that appear similar by optical coherence tomography. The optical coherence tomography microstructural image is surrounded by the near infrared spectroscopy absorption spectrum at each angle of rotation of the catheter, where yellow indicates high absorption (*B* and *C*). The plaque in (*B*) does not exhibit significant near infrared spectroscopy absorption, whereas the lesion in (*C*) does. These near infrared spectroscopy datasets indicate that the plaque in (*B*) is fibrocalcific, whereas in (*C*) is a lipid-rich plaque. Reprinted with permission from Fard *et al.*[53]

conventional pulse-echo measurement (*Figure 6*). An advantage of IVPA imaging—compared with NIRS—is its depth resolution which makes it possible to know the exact spatial location and volume of the lipids within the plaque relative to the lumen border, imaged by IVUS.

Throughout the past 5 years, several prototypes for hybrid IVUS-IVPA imaging have been presented (*Table 2*). Functionally, an IVPA catheter is similar to an IVUS catheter, with the addition of an optical fibre for delivery of light for exciting the IVPA signal. The optical beam is reflected sideways so it is overlapping with the acoustic beam. Early designs based on rotational IVUS catheters,[54] or phased-array transducers[55] were relatively large. They were followed by miniaturized probes that could be used for intracoronary scanning, with high-frequency transducers allowing a very high image resolution of 35 µm.[56] Recently, flexible catheters, suitable for real-time imaging were demonstrated, bringing the image acquisition time to a level with current commercial IVUS systems.[57,58] In the future, extensions to triple-modality IVPA-IVUS-OCT combinations are conceivable.

The first *in vivo* applications of IVPA[59,60] have provided evidence that this modality can become a powerful tool for assessing plaque vulnerability, and quantifying the response to different forms of intervention (device, pharmacologic, and lifestyle changes) with high chemical detail, enabled by multi-wavelength IVPA imaging.[61,62] Nevertheless there is a need to tackle several technical and regulatory hurdles before it can be translated to the clinical arena.[63] Other limitations of the available designs are: the need for blood clearance as blood causes signal attenuation, and the limited ability of IVPA to visualize the entire plaque for quantification of lipid content in the presence of large lipid cores.

Combined fluorescence lifetime imaging-intravascular ultrasound

Recent studies have demonstrated that the fluorescence lifetime values retrieved from point-spectroscopy TRFS or FLIm measurements of diseased arteries can be associated with pathological changes in the intima (~250–300 µm depth) including accumulation of lipid both

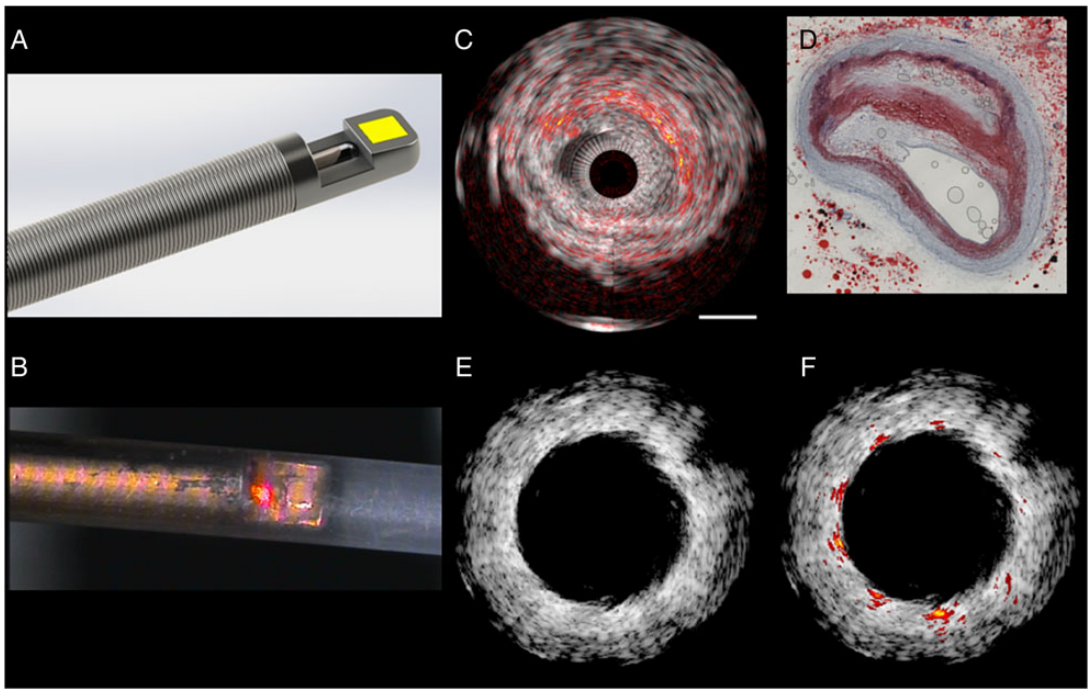

Figure 6 Intravascular ultrasound - intravascular photoacoustic imaging. (*A*) Sketch of a catheter tip, showing the ultrasound transducer (yellow) aligned with the tip of a side-looking optical fibre on a flexible drive shaft. (*B*) Microphotograph of an experimental catheter device (figure provided by M. Wu and G. Springeling unpublished), with a red pointer laser indicating the optical channel, in a polymer sheath (outer diameter 1.1 mm). (*C*) Lipid imaging of a human atherosclerotic plaque ex vivo, wavelength = 1710 nm. Conventional intravascular ultrasound is shown in greyscale, with intravascular photoacoustic lipid signal in red-orange overlay. Comparison with histology (*D*; Oil Red O stain) shows high intravascular photoacoustic signal in lipid-rich areas. (*E*) Stent imaging with intravascular ultrasound in an atherosclerotic vessel with highly echogenic plaque. The stent struts provide very limited contrast. (*F*) The high intravascular photoacoustic signal generated by the metal stent struts allows accurate assessment of stent apposition (J. Su, unpublished).

intracellular (in macrophages) and extracellular (lipid pool), collagen, and elastin and thus enable differentiation between TCFA and tick cap fibroatheromas among other pathological features.[64,65] This lead to the development of several hybrid intravascular catheters combining multispectral rotational FLIm and IVUS for cardiovascular imaging applications, which allows for simultaneous imaging of both biochemical and morphological features of the vessel wall (*Table 2*).

Bec *et al.* reported a rotary catheter that enables simultaneous multispectral FLIm and IVUS imaging. This first prototype had a rather large diameter (7 Fr) that is not feasible for intravascular imaging.[66] Extending on this work, Ma *et al.* reported a fully automated and integrated FLIm-IVUS bimodal miniaturised (3.5 Fr diameter) imaging system compatible with intravascular fast imaging of coronary arteries.[67] In this design, the optic fibre and IVUS transducer were placed in parallel in a large oval shaped shaft (largest diameter of 5 Fr) able to accommodate both of them (*Figure 7A*). The ultrasound and optical channels consist of the imaging elements of the commercial IVUS 3 Fr catheter and a custom, total internal reflection, side-viewing fibre built around a UV-grade silica fibre optic with a polymethylmethacrylate (PMMA) cap (*Figure 7B*). Each modality can be moved into the imaging section and acquire data through helical scanning, while the other inactive channel is pulled back in the shaft. Using the bi-modal catheter described above *ex vivo* intraluminal evaluation of diseased coronary arteries from 16 patients demonstrated that combined FLIm-IVUS imaging was able to distinguish different plaque types with a higher sensitivity and specificity (89%, 99%) than standalone FLIm (70%, 98%) or IVUS (45%, 94%).[68]

The functionality of this system and the ability of FLIm to operate *in vivo* have been tested in a healthy swine left anterior descending coronary artery.[69] The system has been optimized, with particular emphasis on clearing blood from the optical pathway. A short data acquisition time (5 s for a 20 mm long coronary segment) enabled data acquisition during a bolus saline solution injection through a 7 Fr guide catheter. While the mild changes in excitation and collection efficiency, due to vessel geometry and motion that occurred during to cardiac circle, created significant variations of intensity over the field of view that were visible in the intensity images, the computed average lifetime (~6 ns) was uniformly distributed, as expected from a healthy artery (fluorescence dominated by elastin and collagen emission). Due to the cardiac motion the FLIm data could not be directly co-registered with the IVUS data as in *ex vivo* studies.[67,68] This work laid the foundation for further integration of FLIm and IVUS in a device compatible with *in vivo* intravascular imaging (single imaging core, 4 Fr) currently under development

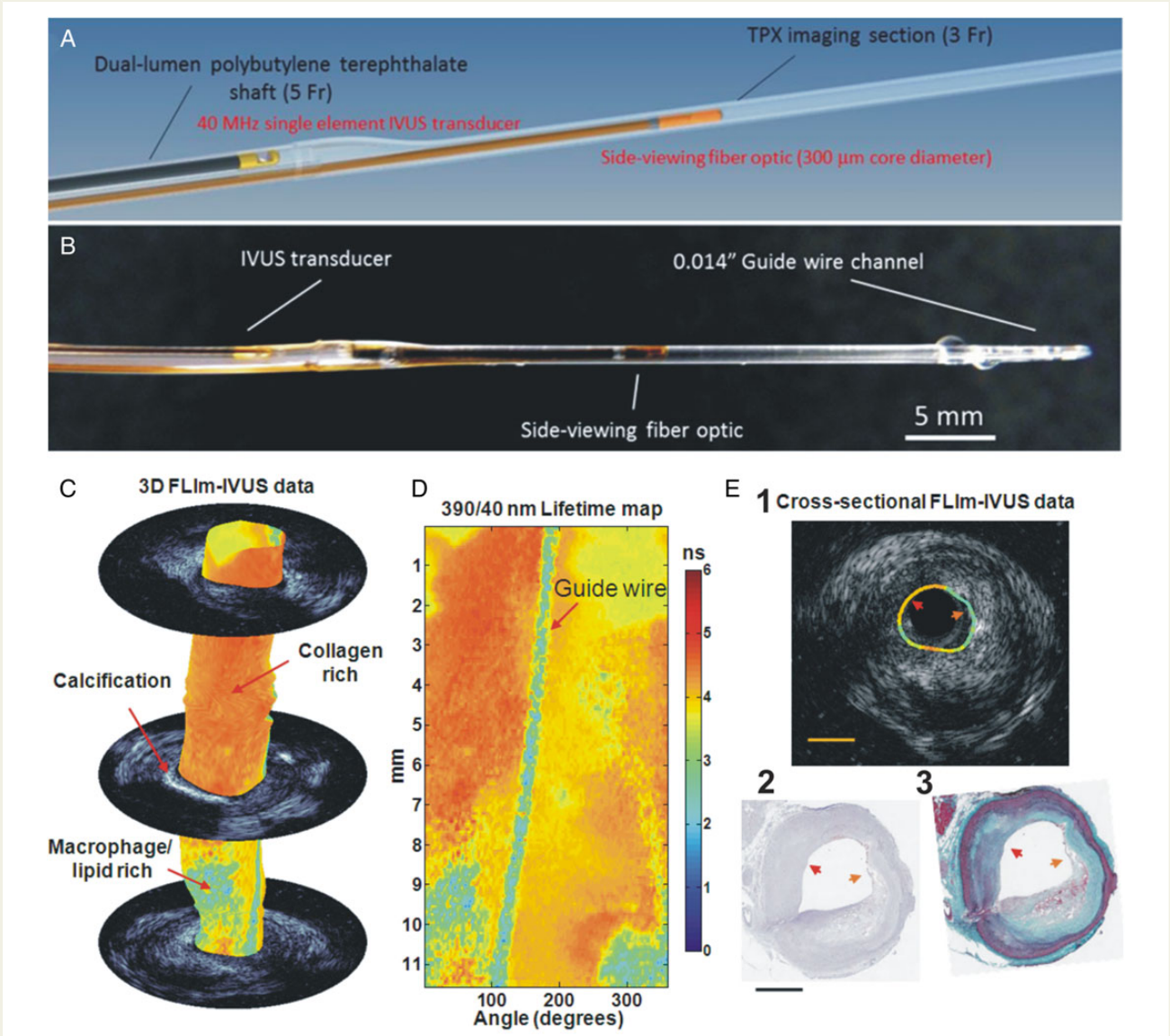

Figure 7 Schematic representation (*A*) and picture (*B*) of the bi-modal intravascular ultrasound-fluorescence lifetime imaging catheter used for the imaging of the coronary arteries. Co-registered fluorescence lifetime imaging-intravascular ultrasound data acquired using a bimodal catheter from an *ex vivo* human coronary artery. Fluorescence lifetime imaging data correspond to lifetime values from 390/40 nm wavelength band. (*C*) Fluorescence lifetime imaging-intravascular ultrasound data in 3D with select intravascular ultrasound frames. (*D*) En-face lifetime map. (*E*) Cross-sectional fluorescence lifetime imaging-intravascular ultrasound data (i) with corresponding (ii) CD68 stained and (iii) elastin-Masson's Trichrome histology sections. Red arrow head points to a region identified as fibrotic (collagen rich) plaque while the orange arrow head points to a region identified as thin-cap fibroatheroma plaque with macrophages (CD68+). Thin-cap fibroatheromas shows lower lifetime when compared with collagen rich areas. Scale bars are 1 mm.

by the Marcu group (UC Davis). This new catheter very recently has been tested *in vivo* in swine coronaries (manuscript in preparation).

Discussion

Advances in molecular biology, new developments in image and signal processing, and the miniaturization of medical devices have enabled the construction of dual-probe intravascular imaging catheters and the design of computer-based methodologies that can provide comprehensive imaging of coronary pathobiology. Validation studies and clinical applications furnish optimism that these devices will allow comprehensive assessment of the pathophysiological mechanisms associated with plaque growth and enable more accurate detection of vulnerable lesions.[34,35,42] Large-scale studies of atherosclerosis that investigate the potential role of hybrid imaging in detecting high-risk lesions and identifying high-risk patients that may benefit from an aggressive treatment of coronary atherosclerosis, have recently commenced.[70] Catheters combining three or four

different modalities with complementary strengths in assessing lumen and outer vessel wall dimensions (OCT with a higher resolution and IVUS with a higher penetration depth), and composition (TRFS that is sensitive to lipids, collagen, and molecules associated with inflammation in plaque but has limited penetration depth with IVPA that can detect lipids and their location in the plaque or NIRS that is sensible to lipids) are foreseeable in the future.

Nevertheless hybrid intravascular imaging has also significant limitations. The invasive nature of these modalities, the increased cost, and the fact that they are unable to visualize the entire coronary tree and provide a complete assessment of coronary artery pathophysiology are fundamental drawbacks that are expected to limit the applications of hybrid imaging in selected populations. Moreover, the described modalities—apart from the combined NIRS-IVUS catheter—are in their infancy and thus there is limited quantitative data to support their accuracy in assessing plaque characteristics and demonstrate their superiority over standalone imaging.[68] Although there is early evidence demonstrating the added value of multimodality imaging over standalone imaging techniques,[42,71–73] further research and histology-based validation studies are required in order to confirm the theoretical advantages of the hybrid imaging modalities in assessing plaque morphology and composition. Finally, the increased time required to process the acquired data is also likely to affect the broad application of hybrid intravascular imaging in the study of atherosclerosis.

Non-invasive imaging and especially CTCA or combined CTCA-positron emission tomography imaging appears as an attractive alternative for the study of coronary atherosclerosis as it allows assessment of coronary artery pathology in the entire coronary tree, quantification of plaque burden and composition, and identification of plaque inflammation.[74,75] Hybrid intravascular imaging modalities are likely to be used in the future to assess the efficacy of new developments in non-invasive imaging and evaluate their accuracy in assessing plaque pathobiology opening new avenues in the study of atherosclerosis.

Conclusions

Hybrid intravascular imaging introduces a unique opportunity for the study of atherosclerosis. The advanced data fusion methodologies have enabled fast coronary reconstruction and accurate assessment of vessel geometry and plaque distribution, while the numerous multimodal catheters that have been recently introduced appear able to permit detailed and comprehensive assessment of the structure, composition, and biology of the atheroma. Cumulative evidence from their first applications in research indicates that hybrid imaging can provide unique insight about plaque vulnerability and identify lesions that are prone to rupture. Further effort is anticipated in the next years to come that will overcome the limitations of the existing designs allowing their broad applications in the clinical practice and research. Hybrid intravascular imaging has gradually matured and is expected to constitute an advantageous approach for the study of atherosclerosis and the identification of high-risk patients.

Supplementary material

Supplementary material is available at *European Heart Journal* online.

Authors' contributions

C.V.B., F.A.J., F.J.G., G.v.S., S.P.M., B.K.C., A.F., L.M., and P.W.S. drafted the manuscript. E.T., Y.Z., A.F.W.S., S.E., J.M., P.H.S., and G.J.T. made critical revision of the manuscript for key intellectual content.

Funding

F.A.J.: NIH R01-HL122388, and AHA Grant #13GRNT17060040.

Conflict of interest: F.A.J. receives sponsored research from Merck, Kowa, and Siemens, and non-financial research support from Boston Scientific. B.K.C. is the CEO of Covani Medical Inc., receives a salary from Covani, is a co-inventor on hybrid IVUS-OCT technologies, and thus may receive royalty income from this technology and has a significant ownership interest in Covani. S.M. is current employee of InfraReDx while J.M. is a consultant of InfraReDx. G.J.T. receives catheter materials from Terumo Corporation. G.J.T. also receives sponsored research funding from Canon Inc. Massachusetts General Hospital has a licensing arrangement with Terumo Corporation, and F.A.J. and G.J.T. have the rights to receive royalties as part of this licensing arrangement.

References

1. Potkin BN, Bartorelli AL, Gessert JM, Neville RF, Almagor Y, Roberts WC, Leon MB. Coronary artery imaging with intravascular high-frequency ultrasound. *Circulation* 1990;**81**:1575–1585.
2. Sano K, Kawasaki M, Ishihara Y, Okubo M, Tsuchiya K, Nishigaki K, Zhou X, Minatoguchi S, Fujita H, Fujiwara H. Assessment of vulnerable plaques causing acute coronary syndrome using integrated backscatter intravascular ultrasound. *J Am Coll Cardiol* 2006;**47**:734–741.
3. Uemura S, Ishigami K, Soeda T, Okayama S, Sung JH, Nakagawa H, Somekawa S, Takeda Y, Kawata H, Horii M, Saito Y. Thin-cap fibroatheroma and microchannel findings in optical coherence tomography correlate with subsequent progression of coronary atheromatous plaques. *Eur Heart J* 2012;**33**:78–85.
4. Pu J, Mintz GS, Biro S, Lee JB, Sum ST, Madden SP, Burke AP, Zhang P, He B, Goldstein JA, Stone GW, Muller JE, Virmani R, Maehara A. Insights into echo-attenuated plaques, echolucent plaques, and plaques with spotty calcification: novel findings from comparisons among intravascular ultrasound, near-infrared spectroscopy, and pathological histology in 2,294 human coronary artery segments. *J Am Coll Cardiol* 2014;**63**:2220–2233.
5. Manfrini O, Mont E, Leone O, Arbustini E, Eusebi V, Virmani R, Bugiardini R. Sources of error and interpretation of plaque morphology by optical coherence tomography. *Am J Cardiol* 2006;**98**:156–159.
6. Stone GW, Maehara A, Lansky AJ, de Bruyne B, Cristea E, Mintz GS, Mehran R, McPherson J, Farhat N, Marso SP, Parise H, Templin B, White R, Zhang Z, Serruys PW. A prospective natural-history study of coronary atherosclerosis. *N Engl J Med* 2011;**364**:226–235.
7. Stone PH, Saito S, Takahashi S, Makita Y, Nakamura S, Kawasaki T, Takahashi A, Katsuki T, Namiki A, Hirohata A, Matsumura T, Yamazaki S, Yokoi H, Tanaka S, Otsuji S, Yoshimachi F, Honye J, Harwood D, Reitman M, Coskun AU, Papafaklis MI, Feldman CL. Prediction of progression of coronary artery disease and clinical outcomes using vascular profiling of endothelial shear stress and arterial plaque characteristics: the PREDICTION Study. *Circulation* 2012;**126**:172–181.
8. Bourantas CV, Garcia-Garcia HM, Naka KK, Sakellarios A, Athanasiou L, Fotiadis DI, Michalis LK, Serruys PW. Hybrid intravascular imaging: current applications and prospective potential in the study of coronary atherosclerosis. *J Am Coll Cardiol* 2013;**61**:1369–1378.
9. Bourantas CV, Kourtis IC, Plissiti ME, Fotiadis DI, Katsouras CS, Papafaklis MI, Michalis LK. A method for 3D reconstruction of coronary arteries using biplane angiography and intravascular ultrasound images. *Comput Med Imaging Graph* 2005;**29**:597–606.
10. Slager CJ, Wentzel JJ, Schuurbiers JC, Oomen JA, Kloet J, Krams R, von Birgelen C, van der Giessen WJ, Serruys PW, de Feyter PJ. True 3-dimensional reconstruction of coronary arteries in patients by fusion of angiography and IVUS (ANGUS) and its quantitative validation. *Circulation* 2000;**102**:511–516.
11. Wahle A, Prause PM, DeJong SC, Sonka M. Geometrically correct 3-D reconstruction of intravascular ultrasound images by fusion with biplane angiography – methods and validation. *IEEE Trans Med Imaging* 1999;**18**:686–699.

12. Bourantas CV, Papafaklis MI, Athanasiou L, Kalatzis FG, Naka KK, Siogkas PK, Takahashi S, Saito S, Fotiadis DI, Feldman CL, Stone PH, Michalis LK. A new methodology for accurate 3-dimensional coronary artery reconstruction using routine intravascular ultrasound and angiographic data: implications for widespread assessment of endothelial shear stress in humans. *EuroIntervention* 2013;**9**:582–593.
13. Bourantas CV, Raber L, Zaugg S, Sakellarios A, Taniwaki M, Heg D, Moschovitis A, Radu M, Papafaklis MI, Kalatzis F, Naka KK, Fotiadis DI, Michalis LK, Serruys PW, Garcia Garcia HM, Windecker S. Impact of local endothelial shear stress on neointima and plaque following stent implantation in patients with ST-elevation myocardial infarction: A subgroup-analysis of the COMFORTABLE AMI-IBIS 4 trial. *Int J Cardiol* 2015;**186**:178–185.
14. Koskinas KC, Feldman CL, Chatzizisis YS, Coskun AU, Jonas M, Maynard C, Baker AB, Papafaklis MI, Edelman ER, Stone PH. Natural history of experimental coronary atherosclerosis and vascular remodeling in relation to endothelial shear stress: a serial, in vivo intravascular ultrasound study. *Circulation* 2010;**121**: 2092–2101.
15. Stone PH, Coskun AU, Kinlay S, Popma JJ, Sonka M, Wahle A, Yeghiazarians Y, Maynard C, Kuntz RE, Feldman CL. Regions of low endothelial shear stress are the sites where coronary plaque progresses and vascular remodelling occurs in humans: an in vivo serial study. *Eur Heart J* 2007;**28**:705–710.
16. Papafaklis MI, Bourantas CV, Theodorakis PE, Katsouras CS, Naka KK, Fotiadis DI, Michalis LK. The effect of shear stress on neointimal response following sirolimus- and paclitaxel-eluting stent implantation compared with bare-metal stents in humans. *JACC Cardiovasc Interv* 2010;**3**:1181–1189.
17. Papafaklis MI, Bourantas CV, Yonetsu T, Vergallo R, Kotsia A, Nakatani S, Lakkas LS, Athanasiou LS, Naka KK, Fotiadis DI, Feldman CL, Stone PH, Serruys PW, Jang IK, Michalis LK. Anatomically correct three-dimensional coronary artery reconstruction using frequency domain optical coherence tomographic and angiographic data: head-to-head comparison with intravascular ultrasound for endothelial shear stress assessment in humans. *EuroIntervention* 2015;**11**:407–415.
18. Toutouzas K, Chatzizisis YS, Riga M, Giannopoulos A, Antoniadis AP, Tu S, Fujino Y, Mitsouras D, Doulaverakis C, Tsampoulatidis I, Koutkias VG, Bouki K, Li Y, Chouvarda I, Cheimariotis G, Maglaveras N, Kompatsiaris I, Nakamura S, Reiber JH, Rybicki F, Karvounis H, Stefanadis C, Tousoulis D, Giannoglou GD. Accurate and reproducible reconstruction of coronary arteries and endothelial shear stress calculation using 3D OCT: comparative study to 3D IVUS and 3D QCA. *Atherosclerosis* 2015;**240**:510–519.
19. Li Y, Gutierrez-Chico JL, Holm NR, Yang W, Hebsgaard L, Christiansen EH, Maeng M, Lassen JF, Yan F, Reiber JH, Tu S. Impact of side branch modeling on computation of endothelial shear stress in coronary artery disease: coronary tree reconstruction by fusion of 3D angiography and OCT. *J Am Coll Cardiol* 2015;**66**: 125–135.
20. Bourantas CV, Papafaklis MI, Kotsia A, Farooq V, Muramatsu T, Gomez-Lara J, Zhang YJ, Iqbal J, Kalatzis FG, Naka KK, Fotiadis DI, Dorange C, Wang J, Rapoza R, Garcia-Garcia HM, Onuma Y, Michalis LK, Serruys PW. Effect of the endothelial shear stress patterns on neointimal proliferation following drug-eluting bioresorbable vascular scaffold implantation: an optical coherence tomography study. *JACC Cardiovasc Interv* 2014;**7**:315–324.
21. Vergallo R, Papafaklis MI, Yonetsu T, Bourantas CV, Andreou I, Wang Z, Fujimoto JG, McNulty I, Lee H, Biasucci LM, Crea F, Feldman CL, Michalis LK, Stone PH, Jang IK. Endothelial shear stress and coronary plaque characteristics in humans: combined frequency-domain optical coherence tomography and computational fluid dynamics study. *Circ Cardiovasc Imaging* 2014;**7**:905–911.
22. Papafaklis MI, Vergallo R, Jia H, Bourantas C, Yonetsu T, Lakkas L, McNulty I, Kotsia A, Lee H, Antoniadis A, Yu B, Naka KK, Fotiadis DI, Feldman C, Michalis L, Jang IK, Stone P. Longitudinal distribution of endothelial shear stress along culprit lesions and association with plaque characteristics in patients with acute coronary syndromes: a three-dimensional frequency-domain optical coherence tomography study. *J Am Coll Cardiol* 2013;**62**:B198–B198.
23. Slager CJ, Wentzel JJ, Gijsen FJ, Schuurbiers JC, van der Wal AC, van der Steen AF, Serruys PW. The role of shear stress in the generation of rupture-prone vulnerable plaques. *Nat Clin Pract Cardiovasc Med* 2005;**2**:401–407.
24. Slager CJ, Wentzel JJ, Gijsen FJ, Thury A, van der Wal AC, Schaar JA, Serruys PW. The role of shear stress in the destabilization of vulnerable plaques and related therapeutic implications. *Nat Clin Pract Cardiovasc Med* 2005;**2**:456–464.
25. van der Giessen AG, Schaap M, Gijsen FJ, Groen HC, van Walsum T, Mollet NR, Dijkstra J, van de Vosse FN, Niessen WJ, de Feyter PJ, van der Steen AF, Wentzel JJ. 3D fusion of intravascular ultrasound and coronary computed tomography for in-vivo wall shear stress analysis: a feasibility study. *Int J Cardiovasc Imaging* 2010;**26**: 781–796.
26. Gijsen FJ, Schuurbiers JC, van de Giessen AG, Schaap M, van der Steen AF, Wentzel JJ. 3D reconstruction techniques of human coronary bifurcations for shear stress computations. *J Biomech* 2014;**47**:39–43.
27. Gijsen F, van der Giessen A, van der Steen A, Wentzel J. Shear stress and advanced atherosclerosis in human coronary arteries. *J Biomech* 2013;**46**(2):240–7.
28. Hetterich H, Jaber A, Gehring M, Curta A, Bamberg F, Filipovic N, Rieber J. Coronary computed tomography angiography based assessment of endothelial shear stress and its association with atherosclerotic plaque distribution in-vivo. *PLoS ONE* 2015;**10**:e0115408.
29. Mortier P, Wentzel JJ, De Santis G, Chiastra C, Migliavacca F, De Beule M, Louvard Y, Dubini G. Patient-specific computer modelling of coronary bifurcation stenting: the John Doe programme. *EuroIntervention* 2015;**11**(Suppl. V):V35–V39.
30. Karanasos A, Schuurbiers JC, Garcia-Garcia HM, Simsek C, Onuma Y, Serruys PW, Zijlstra F, van Geuns RJ, Regar E, Wentzel JJ. Association of wall shear stress with long-term vascular healing response following bioresorbable vascular scaffold implantation. *Int J Cardiol* 2015;**191**:279–283.
31. Gardner CM, Tan H, Hull EL, Lisauskas JB, Sum ST, Meese TM, Jiang C, Madden SP, Caplan JD, Burke AP, Virmani R, Goldstein J, Muller JE. Detection of lipid core coronary plaques in autopsy specimens with a novel catheter-based near-infrared spectroscopy system. *JACC Cardiovasc Imaging* 2008;**1**:638–648.
32. Kini AS, Baber U, Kovacic JC, Limaye A, Ali ZA, Sweeny J, Maehara A, Mehran R, Dangas G, Mintz GS, Fuster V, Narula J, Sharma SK, Moreno PR. Changes in plaque lipid content after short-term intensive versus standard statin therapy: the YELLOW trial (reduction in yellow plaque by aggressive lipid-lowering therapy). *J Am Coll Cardiol* 2013;**62**:21–29.
33. Simsek C, Garcia-Garcia HM, van Geuns RJ, Magro M, Girasis C, van Mieghem N, Lenzen M, de Boer S, Regar E, van der Giessen W, Raichlen J, Duckers HJ, Zijlstra F, van der Steen T, Boersma E, Serruys PW. The ability of high dose rosuvastatin to improve plaque composition in non-intervened coronary arteries: rationale and design of the Integrated Biomarker and Imaging Study-3 (IBIS-3). *EuroIntervention* 2012;**8**:235–241.
34. Madder RD, Husaini M, Davis AT, Van Oosterhout S, Harnek J, Gotberg M, Erlinge D. Detection by near-infrared spectroscopy of large lipid cores at culprit sites in patients with non-ST-segment elevation myocardial infarction and unstable angina. *Catheter Cardiovasc Interv* 2015;**86**:1014–1021.
35. Madder RD, Goldstein JA, Madden SP, Puri R, Wolski K, Hendricks M, Sum ST, Kini A, Sharma S, Rizik D, Brilakis ES, Shunk KA, Petersen J, Weisz G, Virmani R, Nicholls SJ, Maehara A, Mintz GS, Stone GW, Muller JE. Detection by near-infrared spectroscopy of large lipid core plaques at culprit sites in patients with acute ST-segment elevation myocardial infarction. *JACC Cardiovasc Interv* 2013;**6**: 838–846.
36. Oemrawsingh RM, Cheng JM, Garcia-Garcia HM, van Geuns RJ, de Boer SP, Simsek C, Kardys I, Lenzen MJ, van Domburg RT, Regar E, Serruys PW, Akkerhuis KM, Boersma E. Near-infrared spectroscopy predicts cardiovascular outcome in patients with coronary artery disease. *J Am Coll Cardiol* 2014;**64**: 2510–2518.
37. Yin J, Yang HC, Li X, Zhang J, Zhou Q, Hu C, Shung KK, Chen Z. Integrated intravascular optical coherence tomography ultrasound imaging system. *J Biomed Opt* 2010;**15**:010512.
38. Li BH, Leung AS, Soong A, Munding CE, Lee H, Thind AS, Munce NR, Wright GA, Rowsell CH, Yang VX, Strauss BH, Foster FS, Courtney BK. Hybrid intravascular ultrasound and optical coherence tomography catheter for imaging of coronary atherosclerosis. *Catheter Cardiovasc Interv* 2013;**81**:494–507.
39. Yin J, Li X, Jing J, Li J, Mukai D, Mahon S, Edris A, Hoang K, Shung KK, Brenner M, Narula J, Zhou Q, Chen Z. Novel combined miniature optical coherence tomography ultrasound probe for in vivo intravascular imaging. *J Biomed Opt* 2011;**16**: 060505.
40. Li J, Ma T, Jing J, Zhang J, Patel PM, Kirk Shung K, Zhou Q, Chen Z. Miniature optical coherence tomography-ultrasound probe for automatically coregistered three-dimensional intracoronary imaging with real-time display. *J Biomed Opt* 2013;**18**: 100502.
41. Liang S, Ma T, Jing J, Li X, Li J, Shung KK, Zhou Q, Zhang J, Chen Z. Trimodality imaging system and intravascular endoscopic probe: combined optical coherence tomography, fluorescence imaging and ultrasound imaging. *Opt Lett* 2014;**39**: 6652–6655.
42. Fujii K, Hao H, Shibuya M, Imanaka T, Fukunaga M, Miki K, Tamaru H, Sawada H, Naito Y, Ohyanagi M, Hirota S, Masuyama T. Accuracy of OCT, grayscale IVUS, and their combination for the diagnosis of coronary TCFA: an ex vivo validation study. *JACC Cardiovasc Imaging* 2015;**8**:451–460.
43. Jaffer FA, Calfon MA, Rosenthal A, Mallas G, Razansky RN, Mauskapf A, Weissleder R, Libby P, Ntziachristos V. Two-dimensional intravascular near-infrared fluorescence molecular imaging of inflammation in atherosclerosis and stent-induced vascular injury. *J Am Coll Cardiol* 2011;**57**:2516–2526.
44. Yoo H, Kim JW, Shishkov M, Namati E, Morse T, Shubochkin R, McCarthy JR, Ntziachristos V, Bouma BE, Jaffer FA, Tearney GJ. Intra-arterial catheter for simultaneous microstructural and molecular imaging in vivo. *Nat Med* 2011;**17**: 1680–1684.

45. Lee S, Lee MW, Cho HS, Song JW, Nam HS, Oh DJ, Park K, Oh WY, Yoo H, Kim JW. Fully integrated high-speed intravascular optical coherence tomography/near-infrared fluorescence structural/molecular imaging in vivo using a clinically available near-infrared fluorescence-emitting indocyanine green to detect inflamed lipid-rich atheromata in coronary-sized vessels. *Circ Cardiovasc Interv* 2014;**7**:560–569.
46. Vinegoni C, Botnaru I, Aikawa E, Calfon MA, Iwamoto Y, Folco EJ, Ntziachristos V, Weissleder R, Libby P, Jaffer FA. Indocyanine green enables near-infrared fluorescence imaging of lipid-rich, inflamed atherosclerotic plaques. *Sci Transl Med* 2011;**3**:84ra45.
47. Verjans JW, Osborn EA, Ughi G, Calfon MA, Hamidi E, Anotniadis AP, Papafaklis MI, Confrad MF, Libby P, Stone PH, Campria RP, Tearney GJ, Jaffer FA. Clinical and intracoronary evaluation of indocyanine green for targeted near-infrared fluorescence imaging of atherosclerosis. *JACC Cardiovasc Imaging* 2016;in press.
48. Osborn EA, Jaffer FA. The advancing clinical impact of molecular imaging in CVD. *JACC Cardiovasc Imaging* 2013;**6**:1327–1341.
49. Hara T, Ughi GJ, McCarthy JR, Erdem SS, Mauskapf A, Lyon SC, Fard AM, Edelman ER, Tearney GJ, Jaffer FA. Intravascular fibrin molecular imaging improves the detection of unhealed stents assessed by optical coherence tomography in vivo. *Eur Heart J* 2015.
50. Ughi G, Wang H, Gardecki JA, Gerbaud E, Fard AM, Hamidi E, Jacques-Vacas P, Rosenberg M, Jaffer FA, Tearney GJ. First-in-human dual-modality OCT and near-infrared autofluorescence imaging of coronary artery disease. *JACC Cardiovasc Imaging* 2016 (in press).
51. Wang H, Gardecki JA, Ughi GJ, Jacques PV, Hamidi E, Tearney GJ. Ex vivo catheter-based imaging of coronary atherosclerosis using multimodality OCT and NIRAF excited at 633nm. *Biomed Opt Express* 2015;**6**:1363–1375.
52. Dixon AJ, Hossack JA. Intravascular near-infrared fluorescence catheter with ultrasound guidance and blood attenuation correction. *J Biomed Opt* 2013;**18**:56009.
53. Fard AM, Vacas-Jacques P, Hamidi E, Wang H, Carruth RW, Gardecki JA, Tearney GJ. Optical coherence tomography – near infrared spectroscopy system and catheter for intravascular imaging. *Opt Express* 2013;**21**:30849–30858.
54. Karpiouk AB, Wang B, Emelianov SY. Development of a catheter for combined intravascular ultrasound and photoacoustic imaging. *Rev Sci Instrum* 2010;**81**:014901.
55. Hsieh BY, Chen SL, Ling T, Guo LJ, Li PC. Integrated intravascular ultrasound and photoacoustic imaging scan head. *Opt Lett* 2010;**35**:2892–2894.
56. Li X, Wei W, Zhou Q, Shung KK, Chen Z. Intravascular photoacoustic imaging at 35 and 80MHz. *J Biomed Opt* 2012;**17**:106005.
57. Li Y, Gong X, Liu C, Lin R, Hau W, Bai X, Song L. High-speed intravascular spectroscopic photoacoustic imaging at 1000 A-lines per second with a 0.9-mm diameter catheter. *J Biomed Opt* 2015;**20**:065006.
58. Wang P, Ma T, Slipchenko MN, Liang S, Hui J, Shung KK, Roy S, Sturek M, Zhou Q, Chen Z, Cheng JX. High-speed intravascular photoacoustic imaging of lipid-laden atherosclerotic plaque enabled by a 2-kHz barium nitrite Raman laser. *Sci Rep* 2014;**4**:6889.
59. Wang B, Karpiouk A, Yeager D, Amirian J, Litovsky S, Smalling R, Emelianov S. In vivo intravascular ultrasound-guided photoacoustic imaging of lipid in plaques using an animal model of atherosclerosis. *Ultrasound Med Biol* 2012;**38**:2098–2103.
60. Zhang J, Yang S, Ji X, Zhou Q, Xing D. Characterization of lipid-rich aortic plaques by intravascular photoacoustic tomography: ex vivo and in vivo validation in a rabbit atherosclerosis model with histologic correlation. *J Am Coll Cardiol* 2014;**64**:385–390.
61. Jansen K, van der Steen AF, van Beusekom HM, Oosterhuis JW, van Soest G, Intravascular photoacoustic imaging of human coronary atherosclerosis. *Opt Lett* 2011;**36**:597–599.
62. Jansen K, van der Steen AF, Wu M, van Beusekom HM, Springeling G, Li X, Zhou Q, Shung KK, de Kleijn DP, van Soest G. Spectroscopic intravascular photoacoustic imaging of lipids in atherosclerosis. *J Biomed Opt* 2014;**19**:026006.
63. Jansen K, van Soest G, van der Steen AFW. Intravascular photoacoustic imaging: a new tool for vulnerable plaque identification. *Ultrasound Med Biol* 2014;**40**:1037–1048.
64. Marcu L, Jo JA, Fang Q, Papaioannou T, Reil T, Qiao JH, Baker JD, Freischlag JA, Fishbein MC. Detection of rupture-prone atherosclerotic plaques by time-resolved laser-induced fluorescence spectroscopy. *Atherosclerosis* 2009;**204**:156–164.
65. Marcu L, Fishbein MC, Maarek JM, Grundfest WS. Discrimination of human coronary artery atherosclerotic lipid-rich lesions by time-resolved laser-induced fluorescence spectroscopy. *Arterioscler Thromb Vasc Biol* 2001;**21**:1244–1250.
66. Bec J, Ma DM, Yankelevich DR, Liu J, Ferrier WT, Southard J, Marcu L. Multispectral fluorescence lifetime imaging system for intravascular diagnostics with ultrasound guidance: in vivo validation in swine arteries. *J Biophotonics* 2014;**7**:281–285.
67. Ma D, Bec J, Yankelevich DR, Gorpas D, Fatakdawala H, Marcu L. Rotational multispectral fluorescence lifetime imaging and intravascular ultrasound: bimodal system for intravascular applications. *J Biomed Opt* 2014;**19**:066004.
68. Fatakdawala H, Gorpas D, Bishop JW, Bec J, Ma D, Southard JA, Margulies KB, Marcu L. Fluorescence lifetime imaging combined with conventional intravascular ultrasound for enhanced assessment of atherosclerotic plaques: an ex vivo study in human coronary arteries. *J Cardiovasc Transl Res* 2015;**8**:253–263.
69. Bec J, Ma D, Yankelevich DR, Gorpas D, Ferrier WT, Southard J, Marcu L. In-vivo validation of fluorescence lifetime imaging (FLIm) of coronary arteries in swine. *Photonic Therapeutics and Diagnostics XI, SPIE Proc* 2015;**9303**.
70. Bourantas CV, Garcia-Garcia HM, Torii R, Zhang YJ, Westwood M, Crake T, Serruys PW. Vulnerable plaque detection: an unrealistic quest or a feasible objective with a clinical value? *Heart* 2016.
71. Brown AJ, Obaid DR, Costopoulos C, Parker RA, Calvert PA, Teng Z, Hoole SP, West NE, Goddard M, Bennett MR. Direct comparison of virtual-histology intravascular ultrasound and optical coherence tomography imaging for identification of thin-cap fibroatheroma. *Circ Cardiovasc Imaging* 2015;**8**:e003487.
72. Kang SJ, Mintz GS, Pu J, Sum ST, Madden SP, Burke AP, Xu K, Goldstein JA, Stone GW, Muller JE, Virmani R, Maehara A. Combined IVUS and NIRS detection of fibroatheromas: histopathological validation in human coronary arteries. *JACC Cardiovasc Imaging* 2015;**8**:184–194.
73. Puri R, Madder RD, Madden SP, Sum ST, Wolski K, Muller JE, Andrews J, King KL, Kataoka Y, Uno K, Kapadia SR, Tuzcu EM, Nissen SE, Virmani R, Maehara A, Mintz GS, Nicholls SJ. Near-infrared spectroscopy enhances intravascular ultrasound assessment of vulnerable coronary plaque: a combined pathological and in vivo study. *Arterioscler Thromb Vasc Biol* 2015;**35**:2423–2431.
74. Joshi NV, Vesey AT, Williams MC, Shah AS, Calvert PA, Craighead FH, Yeoh SE, Wallace W, Salter D, Fletcher AM, van Beek EJ, Flapan AD, Uren NG, Behan MW, Cruden NL, Mills NL, Fox KA, Rudd JH, Dweck MR, Newby DE. 18F-fluoride positron emission tomography for identification of ruptured and high-risk coronary atherosclerotic plaques: a prospective clinical trial. *Lancet* 2014;**383**:705–713.
75. Voros S, Rinehart S, Qian Z, Vazquez G, Anderson H, Murrieta L, Wilmer C, Carlson H, Taylor K, Ballard W, Karmpaliotis D, Kalynych A, Brown C 3rd. Prospective validation of standardized, 3-dimensional, quantitative coronary computed tomographic plaque measurements using radiofrequency backscatter intravascular ultrasound as reference standard in intermediate coronary arterial lesions: results from the ATLANTA (assessment of tissue characteristics, lesion morphology, and hemodynamics by angiography with fractional flow reserve, intravascular ultrasound and virtual histology, and noninvasive computed tomography in atherosclerotic plaques) I study. *JACC Cardiovasc Interv* 2011;**4**:198–208.